The Astrophysical Journal, 664:1214–1220, 2007 August 1

THE QUIET SUN NETWORK AT SUBARCSECOND RESOLUTION: VAULT OBSERVATIONS AND RADIATIVE TRANSFER MODELING OF COOL LOOPS

S. Patsourakos[1]
Naval Research Laboratory, Space Science Division, Washington, DC 20375;patsourakos@nrl.navy.mil

P. Gouttebroze
Institut d'Astrophysique Spatiale, Université de Paris XI, Bât. 121, 91405 Orsay, France

and

A. Vourlidas
Code 7663, Naval Research Laboratory, Washington, DC 20375
Received 2007 January 25; accepted 2007 April 2

ABSTRACT

One of the most enigmatic regions of the solar atmosphere is the transition region (TR), corresponding to plasmas with temperatures intermediate of the cool, few thousand K, chromosphere and the hot, few million K, corona. The traditional view is that the TR emission originates from a thin thermal interface in hot coronal structures, connecting their chromosphere with their corona. This paradigm fails badly for cool plasmas ($\approx T < 10^5$ K), since it predicts emission orders of magnitude less than what it is observed. It was therefore proposed that the "missing" TR emission could originate from tiny, isolated from the hot corona, cool loops at TR temperatures. A major problem in investigating this proposal is the very small sizes of the hypothesized cool loops. Here, we report the first spatially resolved observations of subarcsecond-scale looplike structures seen in the Lyα line made by the Very High Angular Resolution Ultraviolet Telescope (VAULT). The subarcsecond ($\approx 0.3''$) resolution of VAULT allows us to directly view and resolve looplike structures in the quiet Sun network. We compare the observed intensities of these structures with simplified radiative transfer models of cool loops. The reasonable agreement between the models and the observations indicates that an explanation of the observed fine structure in terms of cool loops is plausible.

Subject headings: Sun: transition region

Online material: color figures

1. INTRODUCTION

Solar plasmas with temperatures between these of the chromosphere and the corona are defined as the transition region (TR). Despite intense efforts over the last decades, the structure of the transition region remains highly uncertain (e.g., Mariska 1992). One of the major problems of TR physics is the "missing" differential emission measure (DEM) in the lower TR corresponding to $\approx T < 10^5$ K. Traditional models (e.g., Gabriel 1976; Athay 1981), assuming that the TR emission originates from the bases of large-scale structures reaching coronal temperatures at their upper sections, predict a DEM that is orders of magnitude smaller than the observed DEM (for a review see Mariska 1992). Therefore, Dowdy et al. (1986) proposed that the lower transition region has a second structural component: very small cool loops that do not reach coronal temperatures. A suitable mixture of cool loops with different temperatures, and maybe in a dynamic state, can account for the "missing" lower transition region DEM (e.g., Antiochos & Noci 1986; Peter et al. 2004; Spadaro et al. 2006). Very suggestive' recent subarcsecond ($\approx 0.1''$) resolution photospheric magnetic field observations reveal a multitude of fluxtube-like concentrations over the quiet Sun network (Berger et al. 2004). It is conceivable then that these flux tubes could close down to the photosphere on scales of few thousand km (Schrijver & Title 2003; Close et al. 2004; Wiegelmann & Solanki 2004; Tu et al. 2005; Aiouaz & Rast 2006).

There exists significant indirect observational evidence for subresolution TR structure. This includes double-component TR spectra (Peter 2001), spatially and temporally scale-invariant intensity power spectra (e.g., Berghmans et al. 1998) and differential emission measure distributions (e.g., Griffiths et al. 1999), small filling factors and unresolved mass motions (e.g., Dere et al. 1987; Dere & Mason 1993; Chae et al. 1998), small-scale dynamics (e.g., Dere et al. 1987; Dere 1994; Innes et al. 1997; Patsourakos & Vial 2001; Teriaca et al. 2004; Winebarger et al. 2002), temporal and spatial intermittency (Patsourakos & Vial 2002; Buchlin et al. 2006), and arcsecond-scale differences in measured intensities, Doppler and nonthermal velocities in TR lines with different formation temperatures (Akiyama et al. 2005; Doschek et al. 2004; Doschek 2006).

The first observational inferences of the elusive cool loops came from high spatial resolution observations of the transition region from the rocket flights of transition region camera (TRC) and high-resolution telescope and spectrograph (HRTS) and from the SUMER spectrometer on *SOHO* (e.g., Bonnet et al. 1980; Dere et al. 1987; Feldman et al. 1999; Landi et al. 2000). These observations showed the existence of very thin threads, with a thickness of about $1''$–$2''$, straddling the network boundaries. Although quite suggestive, these observations did not resolve the hypothesized arcsecond-scale cool loops.

The problem in determining the TR building blocks arises from the very small horizontal and vertical spatial scales involved. What is therefore needed is at least 1 order of magnitude increase in the spatial resolution, to pinpoint the arcsecond-scale structures described in the previous paragraph, which may then be the elusive cool loops.

[1] Also at Center for Earth Observing and Space Research, Institute for Computational Sciences, George Mason University, Fairfax, VA 22030.

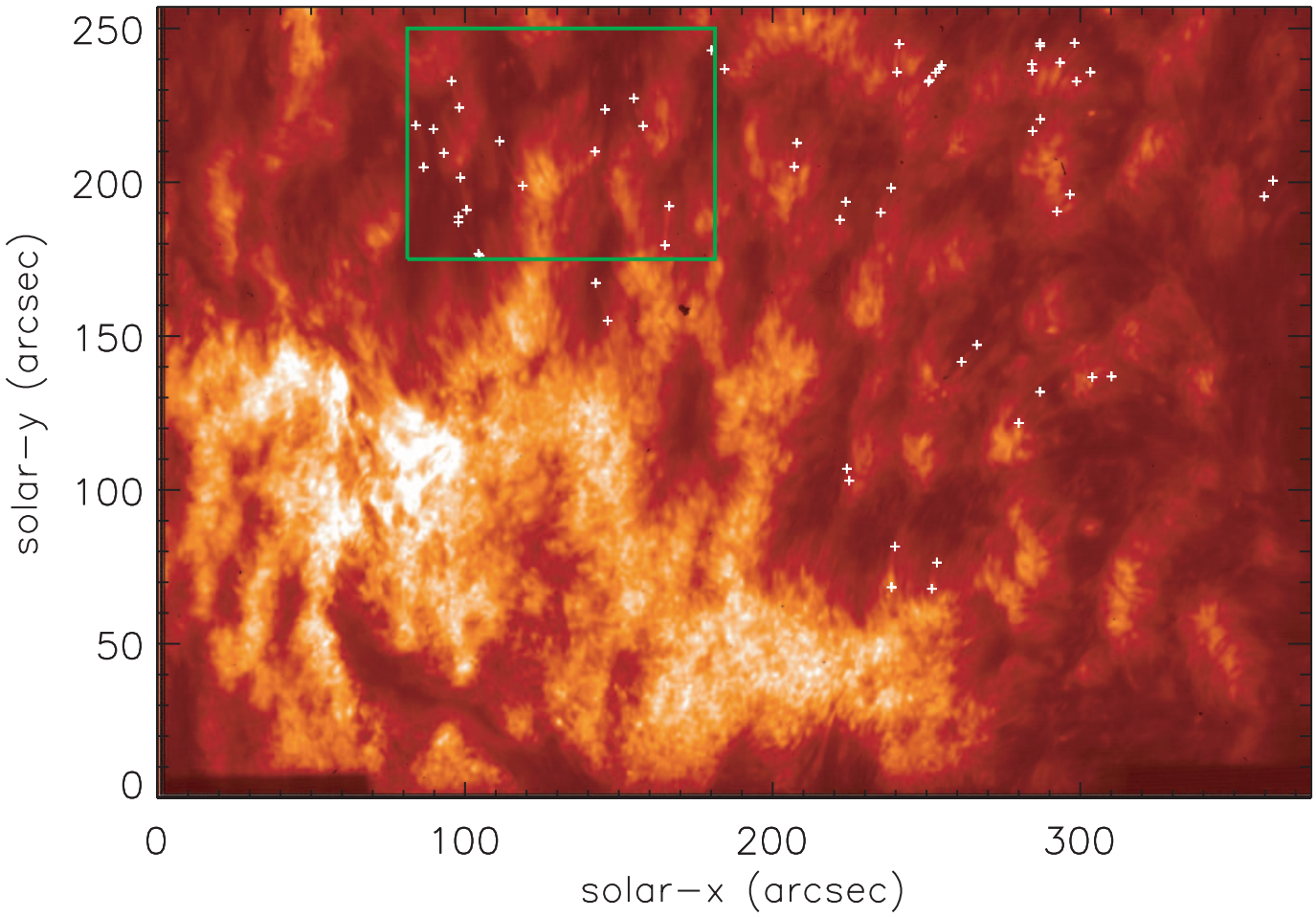

FIG. 1.—VAULT Lyα image used in the analysis. With squares we plot the first and final point used in the tracing of the 33 looplike structures described in § 2. The green box contains a $\approx 100'' \times 60''$ region, covering several supergranulation cells. We plot the square root of the measured intensity. Intensity is represented by color, increasing from black to red to white.

The above requirement has been satisfied with the advent of the Very High Angular Resolution Ultraviolet Telescope (VAULT). In this work we report on the first spatially resolved observations of arcsecond-scale looplike structures in the Lyα line in the quiet Sun. The superior, subarcsecond-spatial resolution of VAULT allowed for the first time viewing of a bounty of very thin, down to the instrument resolution, looplike structures threading the quiet Sun network. With VAULT it was possible to resolve these looplike structures and accurately measure their intensities, which provided the opportunity to compare them with predictions of simplified radiative transfer models of cool loops. We were therefore able to perform the first qualitative test on the existence of TR cool loops.

Our paper is organized as follows: § 2 discusses our observations and their analysis, while § 3 describes the numerical model used to simulate cool loops. Finally, § 4 describes the comparison between the observations and the modeling and gives our conclusions.

2. OBSERVATIONS AND DATA ANALYSIS

We present observations made with the Very High Angular Resolution Angular Telescope (VAULT; Korendyke et al. 2001). VAULT is a Cassegrain telescope feeding a zero-dispersion spectroheliograph. The spectroheliograph is centered at the Lyα line (1216 Å) with a bandpass of around 70 Å, which ensures spectrally pure Lyα images.[2] The UV light from the telescope-spectroheliograph system is imaged on a lumogen-coated 3072×2048 CCD array with $0.125''$ pixels. VAULT achieves a spatial resolution of $\approx 0.3''$. For more on VAULT, the interested reader is referred to Korendyke et al. (2001).

The observations reported here were carried out during the second sounding rocket flight of VAULT on 14 June 2002 around 18:12 UT. The high intrinsic intensity of the Lyα line combined with the high sensitivity of VAULT permitted short exposures of 1 s. The VAULT images were first corrected for bias and dark current. We selected a representative image from this flight for further analysis (Fig 1). It corresponds to a field of view (FOV) of $375'' \times 257''$ centered at $(-600'', 260'')$ from disk center, and an exposure time of 1 s was used. The observed FOV covers mainly quiet Sun areas, although its southeast part corresponds to active region (AR) plage. Our present study is dedicated to the quiet Sun.

The quiet Sun in Figure 1 is dominated by the omnipresent chromospheric network pattern, which is manifested as a mosaic of dark internetwork areas surrounded by bright network boundaries. This was already recognized from the first observations of

[2] The Lyα intensity decreases rapidly in the line wings: it is almost 1/100 and 1/1000 at 1 and 5 Å from line center, respectively (e.g., Lemaire et al. 1998), which means that the contribution of the far wings to the VAULT bandpass can be safely neglected.

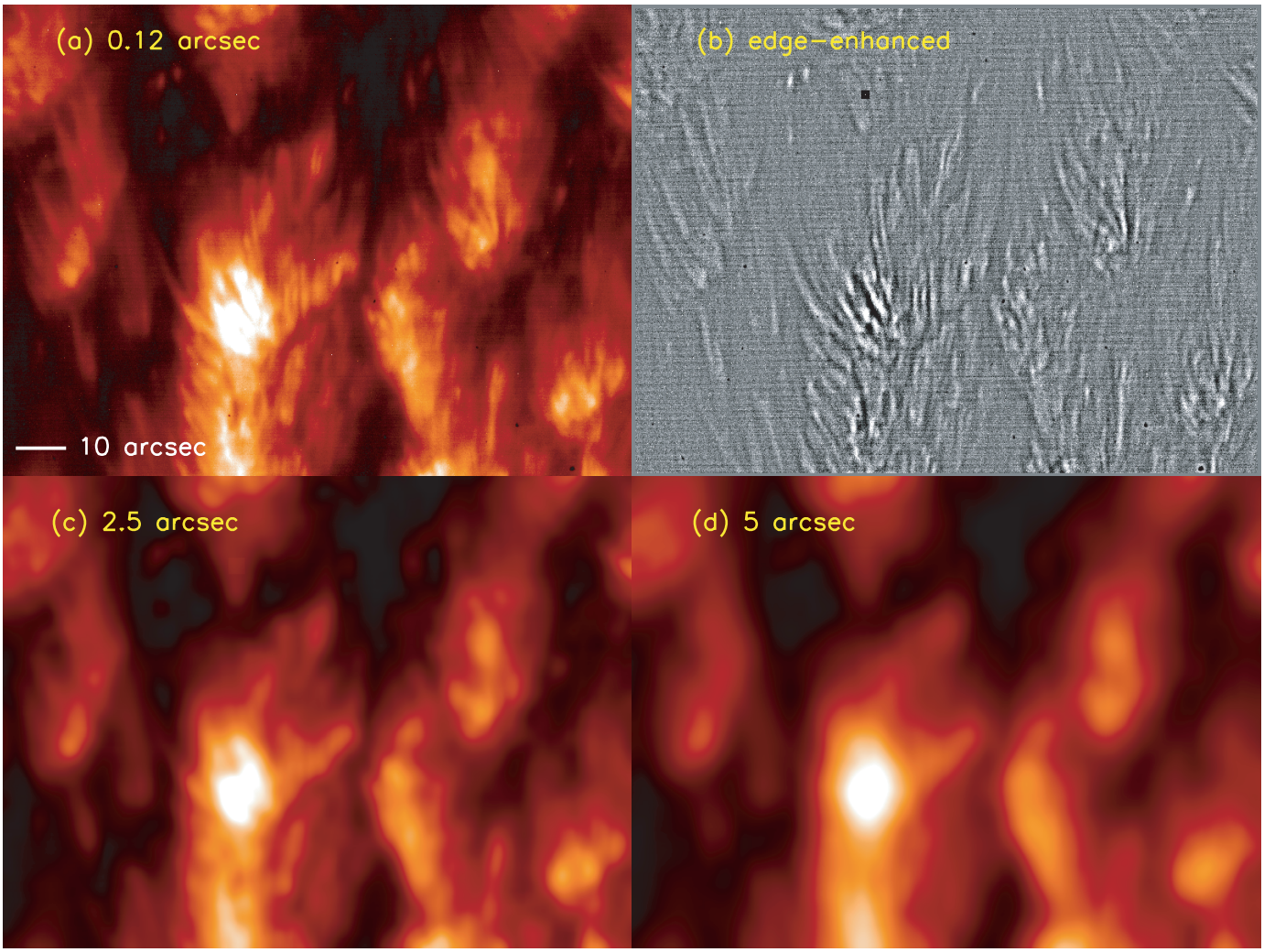

FIG. 2.—VAULT image of a $\approx 100'' \times 60''$ quiet Sun region, enclosed in the green box of Fig. 1. Edge-enhanced version of the original image (*panel b*), highlighting features with a spatial scale of $1.2''$. Panels *c* and *d* contain boxcar smoothed versions of the original image with a window width of 20 and 40 pixels, respectively. We plot the square root of the measured intensity. Intensity is represented by color, increasing from black to red to white.

the quiet Sun in Lyα dating back to the *Skylab* era (e.g., Reaves et al. 1976). However, the superior subarcsecond resolution of VAULT allows us strikingly novel and detailed views of the very fine structure of the network.

It is evident from Figure 1 that the network boundaries are not the rather continuous patch of emission surrounding the internetwork, seen earlier with modest spatial resolution. VAULT images show a forest of very thin structures threading the network. The threadlike structures can be as long as the network thickness (around $10''$ for the lower TR; e.g., Patsourakos et al. 1999; Gontikakis etal. 2003) and have widths in the range of $\approx 1''$–$3''$ down to the instrument resolution. The high spatial resolution of VAULT provides for the first time the opportunity to adequately resolve arcsecond-scale threads in the network, with several pixels both along and across them.

To appreciate and further illustrate the power of high spatial resolution we produced Figure 2. Figure 2*a* contains the subimage inside the green box of Figure 1, while Figure 2*b* is an edge-enhanced version of the image of Figure 2*a*, calculated by subtracting a 10 pixel wide ($\approx 1.2''$) boxcar-smoothed image from the original image. Figures 2*c* and 2*d* contain smoothed versions of the original image with a boxcar width of 20 ($2.5''$) and 40 ($5''$) pixels emulating the spatial smoothing effect of previous network observations made by CDS and *Skylab*, respectively. It clear from this figure that the network is dominated by thin arcsecond-scale structures (Figs. 2*a* and 2*b*). Degrading the spatial resolution (Figs. 2*c* and 2*d*) leads to missing most of the network fine structure by viewing continuous "fat" emission patches around cell centers.

The very high spatial resolution of VAULT provides the opportunity to appreciate the three-dimensional nature of the threads. The threads are, at a first approximation, radially distributed or slightly bent around the cell centers, which suggests that they could correspond to closed structures, i.e., small cool loops with temperatures in the temperature formation region of Lyα. The investigation of this possibility is in fact the chief objective of our paper.

The intensity distribution along the greater part of the threads is more or less uniform, implying an almost constant pressure and temperature along the threads. The pressure should be constant as long as the height of the structure does not greatly exceed the gravitational scale-height (≈ 1500 km for $T = 30{,}000$ K).

For quantitative analysis of the postulated cool loops, we followed a procedure commonly used in the analysis of coronal loops (e.g., Klimchuk 2000). An example of the application of the method is given in Figure 3. The method consists of the following steps. (1) We manually trace the loop axis in the original image (Fig. 3, *upper panel*) and extract a subimage centered at

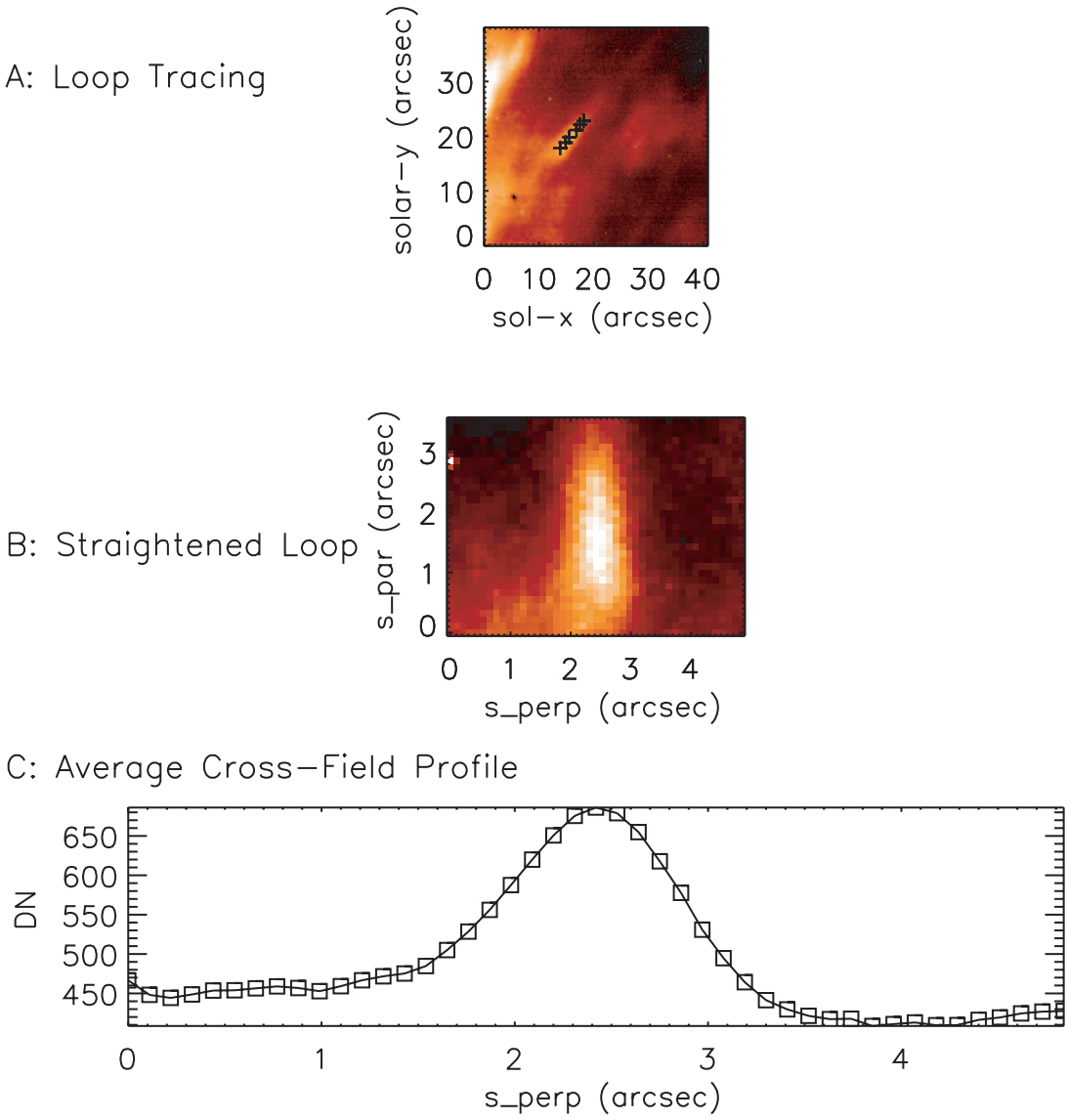

FIG. 3.—Example of the procedure used in the analysis of the Lyα threads described in § 2: (1) loop tracing (*upper panel*), (2) straightening of the loop image in directions parallel and perpendicular to its axis (*middle panel*), and (3) obtaining an average cross-field intensity profile by averaging the straightened image along the loop (*lower panel*; the intensity at each point across the loop is represented by a square). In the upper and middle panel we plot the square root of the measured intensity, which is represented by color, increasing from black to red to white.

the loop axis. (2) We then project the subimage on a new coordinate system running parallel and perpendicular to the loop axis (Fig. 3, *middle panel*), and (3) we average the straightened image intensity along the loop axis, thus obtaining an average cross-field intensity profile (Fig. 3, *lower panel*). The observed fluxes (in DN s^{-1}) were converted to physical units using the radiometric calibration of VAULT. For this task we used an intercalibration study, which compared VAULT intensities with Lyα spectroscopic observations taken by SUMER (L. Teriaca 2007, private communication). The data of each individual data set corresponded to quiet Sun. The central (peak) intensity of the averaged cross-field profile of the lower panel of Figure 3 can be considered as a proxy for the entire loop and will be used in the subsequent comparison with the modeling. From Figure 3 we note that the loop cross-section seems to be constant throughout its length; the FWHM of the intensity cross-field profile is $\approx 1''$, which means that the "real" FWHM of the loop should be $\approx 0.9''$, given that the FWHM of the VAULT point-spread function is $\approx 0.4''$. More than 10 VAULT pixels fit in the cross-section of the loop. The inferred loop FWHM may be even smaller given the intensity cross-field profile of Figure 3 is not perfectly symmetric.

The above procedure was applied to 33 relatively isolated threads, thereby building a decent statistical sample. We note here that finding relatively isolated threads was not easy: very frequently, adjacent threads were so close that it was impossible to separate them. Moreover, it is possible that our sample was biased toward long and bright threads, which are easier to detect than short and faint ones.

In Figure 1 we indicate the tracings for the selected threads by plotting the first and final point of each tracing. The observed threads have FWHM widths in the range of $0.9''$–$2.4''$, lengths in the range of $4''$–$10''$, and (average) intensities in the range of 1.8–5.6×10^5 erg cm^2 s^{-1} sr^{-1} (see also Table 1).

3. MODELING

The problem of modeling the Lyα line is very involved, given its optically thick character. In this work we used a radiative transfer model for cylindrical objects described in Gouttebroze (2004).

TABLE 1
PHYSICAL PARAMETERS OF THE QUIET SUN Lyα THREADS

Parameter	Range
Length (arcsec)	4–10
FWHM width (arcsec)	0.9–2.4
Intensity (erg cm^{-2} s^{-1} sr^{-1})	1.8–5.6 $\times$ 10^5
Temperature (K)	10,000–30,000
Pressure (dyn cm^{-2})	0.1–0.3

NOTE.—Lengths, widths, and intensities are obtained directly from the observations, whereas temperatures and pressures are inferred from the radiative transfer modeling of the observations.

The model solves the non-LTE radiative transfer and statistical equilibrium equations in a cylinder, with external incident radiation. It is assumed that the cylinder has uniform pressure and the external radiation field is isotropic. Temperature is taken as constant in most of the cases. Some models are also computed with a temperature gradient toward the exterior. Moreover, the cylinder does not support mass flows and time-dependent effects. Finally, it is assumed that the cylinder is vertical and sits at an arbitrary altitude above the surface, which enters into the calculation of the dilution factor of the external radiation field. The precise value of the cylinder altitude does not alter the dilution factor given the size of the modeled cylinder is too small compared with the solar radius. For more details on the model the reader is referred to Gouttebroze (2004).

Inclusion of nonisotropic radiation fields (i.e., inclined cylinders) has minimal impact on the predicted Lyα intensities for temperatures >8000 K (Gouttebroze 2005, 2006), which are more relevant to Lyα. The principal effect of inclination is that at low temperatures (<8000 K), scattering is important, and the side of the cylinder turned toward the Sun is brighter than the side turned away. Since this latter side is visible by the observer, the inclination tends to reduce the apparent brightness of the structure. At higher temperatures the main part of the radiation is of thermal origin, so that it becomes isotropic, and the inclination becomes unimportant. Note also that this effect of thermal emission does not occur for very low pressures. However, for such a case, the emitted intensity is too low to match the observations.

These simplifications allow the fast computation of a handful of models in a reasonable CPU time, which gives us the opportunity to thoroughly explore the relevant parameter space. Each model is defined in terms of the cylinder diameter $D_{\rm cyl}$ and (uniform) temperature $T_{\rm cyl}$ and pressure $P_{\rm cyl}$. We calculated models with $D_{\rm cyl} = 700$, 1000, and 1500 km, $P_{\rm cyl} = 0.02$, 0.04, 0.07, 0.1, 0.2, 0.3, 0.5, and 1 dyn cm^{-2}), and $T_{\rm cyl} = 6000$, 8000, 10,000, 12,000, 15,000, 20,000, 25,000, and 30,000 K.

Finally, all our models are characterized by a microturbulent velocity of 5 km s^{-1}, which is consistent with spectroscopic observations of line broadening in the low TR (e.g., Dere & Mason 1993). The incident radiation line profiles used in our modeling were taken from Gouttebroze et al. (1993). The intensities emitted by the threads also depend on a prescribed Lyα background intensity, since these threads are seen on the solar disk. This background intensity represents the nonzero intensity, which would be observed in the absence of the cylinder. For most models, a low background (0.2 times the mean quiet Sun intensity) has been used in order to evidence the emission of the cylinders. However, to obtain a good fit of particular threads, it is generally necessary to use higher background values. This is due to the fact that real threads are seen above other solar structures with comparable intensities, rather than above a dark (i.e., photospheric) background.

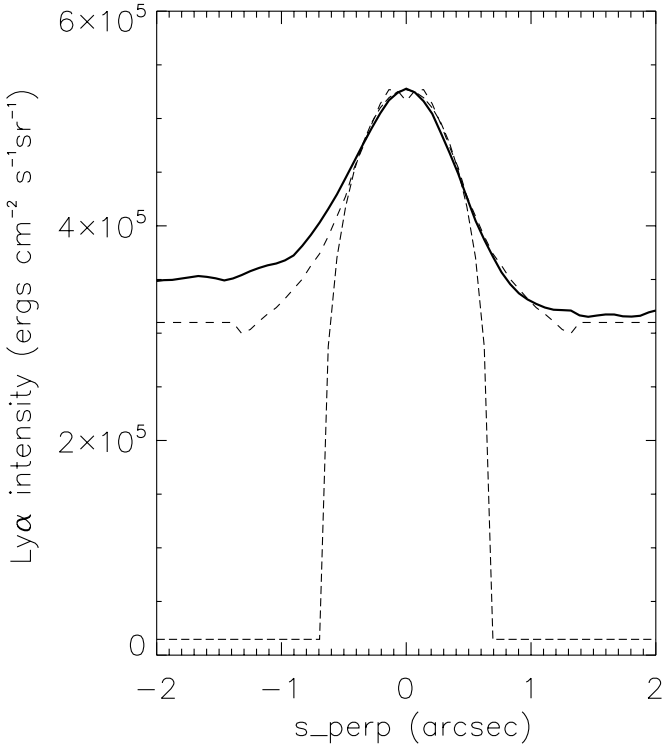

FIG. 4.—Example of the modeling procedure. Cross-field intensity profile for a sample observed loop (*solid line*) and for two radiative transfer models. *Dashed* (*low background level*) *line*: an isobaric isothermal model ($P = 0.35$ dyn cm^{-2}, $T = 20{,}000$ K, $D_{\rm cyl} = 1000$ km) with a low background, which fits the central intensity. *Dashed line*: a model with a pressure of 0.25 dyn cm^{-2} and a temperature gradient toward exterior (axis temperature: 10,000 K, gradient: 40 K km^{-1}, external radius: 1000 km). A high background has been adopted in order to fit the observed one. [*See the electronic edition of the Journal for a color version of this figure.*]

Our modeling therefore provides models of cool cylinders, thermally isolated from the corona, thus approximating cool transition region loops.

The above choice of free parameters reflects a variety of physical conditions, in terms of pressure and temperature, of Lyα emitting structures and of the approximative widths of the observed threads. We have therefore constructed a grid of $3 \times 8 \times 8 = 192$ models. The calculation of each model gave the profile-integrated (total) Lyα intensity as a function of position across the cylinder. For comparison with the observations we use the central intensity of these cross-field profiles.

As an illustration of the modeling procedure, we plot in Figure 4 the cross-field intensity profile for the loop of Figure 3 and for two calculated radiative transfer models. The first model is an isothermal and isobaric cylinder ($T = 20{,}000$ K, $P = 0.35$ dyn cm^{-2}, $D_{\rm cyl} = 1000$ km) with the low background intensity of the previous paragraph. Its pressure is adjusted in order to fit the central intensity of the observed structure. The other model, which produces a better fit of the whole intensity curve, is also isobaric (0.25 dyn cm^{-2}), but its temperature increases linearly from the axis (10,000 K) toward the exterior with a gradient of 40 K km^{-1}. In addition, the background intensity is raised to a relatively high value to reproduce the surrounding observations. This model is limited to a radius of 1000 km, corresponding to $T = 50{,}000$ K, which explains the small discontinuity visible on Figure 4.

4. DISCUSSION AND CONCLUSIONS

The results of the modeling are given in Figure 5, where we plot the central Lyα intensity of each cylindrical model against

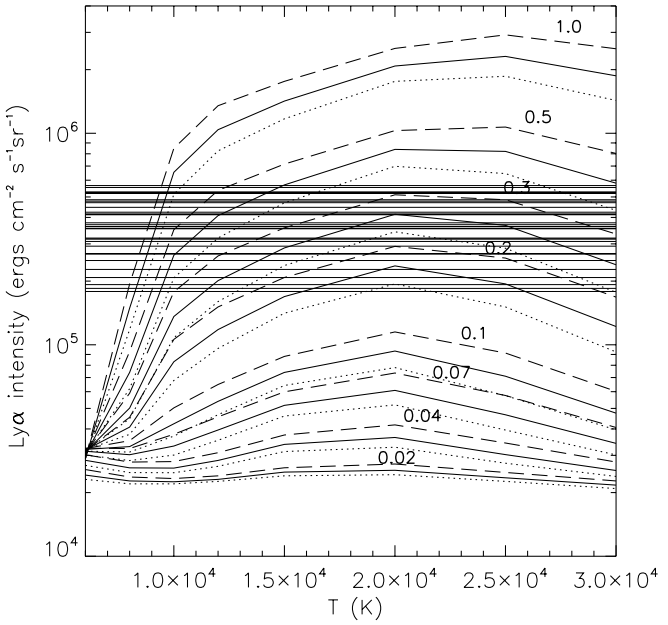

FIG. 5.—Central Lyα intensities predicted by a radiative transfer model for cylinders with a diameter of 700 km (*dotted line*), 1000 km (*solid line*) and 1500 km (*dashed line*) as a function of the cylinder temperature. Each triplet of solutions with different cylinder diameters correspond to a uniform pressure (in dyn cm^{-2}) given on top of each triple (i.e., above the dashed curves). The horizontal solid lines correspond to the intensities of the observed threads. [*See the electronic edition of the Journal for a color version of this figure.*]

its temperature for various values of the cylinder pressure and diameter. The low background value is used for this set of computations. Figure 5 is completed by the central intensities of the observed loops, as determined in § 2.

For a given cylinder temperature, a larger diameter and/or an elevated pressure lead to higher intensities: this is because the Lyα line optical depth increases and so does the line width. For a given pressure and radius of the cylinder, the central intensity peaks at a temperature corresponding to the maximum population of H II. The temperature of maximum central intensity moves to higher temperatures with increasing pressure.

The observed intensities lie in the range $1.8–5.6\times10^5$ erg cm^2 s^{-1} sr^{-1}. The somehow elevated intensity values can be explained by the fact that our observations were carried close to solar maximum, and it is known that the chromospheric and lower transition region quiet Sun emissions, and Lyα in particular, exhibiting a significant increase from a solar minimum to solar maximum (e.g., Schühle et al. 2000; Lemaire et al. 2005). Moreover, the observed quiet Sun area is close to AR plage (e.g., Fig. 1), which means that it could have been the result of AR decay. ARs are characterized by higher pressures and intensities than the "normal" quiet Sun, which also explains the high intensities of the observed quiet Sun structures. The intensities have an uncertainty of $\approx$20% arising from the uncertainties in the photometric calibration of VAULT. The random error, due to photon-counting statistics, is negligible given the high count rates (of several hundred DN per pixel) detected by VAULT.

Figure 5 shows that there are multiple solutions in the sense that each horizontal line, corresponding to the intensity of an observed thread, crosses the intensity curves from our modeling in several points. Multiple solutions can be expected on the grounds that the model, for a given diameter estimated by the observations, depends on two free parameters (temperature and pressure), and there is only one independent variable to constrain them, the intensity. It is not therefore necessary to build "denser" grids of models, which will merely increase the number of the (multiple) solutions. All we can do here is to constrain the solutions in admissible temperature-pressure domains in the solution space. There are no solutions for (low) pressures $<\approx0.07$ dyn cm^{-2}. Moreover, we can exclude a handful of low-temperature ($\approx T < 10{,}000$ K) solutions, because these solutions correspond to rather elevated pressures ($>\approx0.5$ dyn cm^{-2}). Such pressures are typical for the transition region in developed active regions (e.g., Withbroe & Noyes 1977; Tsiropoula et al. 1986; Mariska 1992) and not for the quiet Sun, which is characterized by pressures in the range of $\approx$0.08–0.3 dyn cm^{-2} (Withbroe & Noyes 1977; Fontenla et al. 1991; Mariska 1992; Doschek et al. 1998). We can expect somehow higher pressures for the quiet Sun areas of our study, given their possible association with AR plage as well as the solar maximum conditions of our observations (e.g., the discussion of the previous paragraph).

Having hence excluded solutions with low temperatures/high pressures and solutions with low pressures, we can assert from Figure 5 that the observations are consistent with temperatures of 10,000–30,000 K and pressures of 0.1–0.3 dyn cm^{-2}. This "bracketing" of the observations is very revealing. It means that the VAULT observations of the network fine structure are certainly consistent with cool and thermally isolated from the corona structures, which could then be the elusive cool loops. If these fine structures were instead the footpoints of large-scale structures reaching coronal temperatures, then their emission should have been orders of magnitude smaller than what is observed.

Our results therefore provide significant support for the existence of cool loops in the quiet Sun. The postulated Lyα network loops could then be associated with arch-shaped mottles seen at cooler emissions in the Hα line (e.g., Zachariadis et al. 1999). Note also that we did find some evidence for substantial structure at the resolution limit of VAULT (i.e., 0.3″). However, this does not necessarily imply the scarcity of structure with sizes of 1–2 VAULT pixels. This is because the optical depth of the Lyα lines gets close to unity for subarcsecond structures with typical pressures and temperatures, and therefore the line becomes effectively optically thin. Therefore, the emission from the optically thin subarcsecond loops could be effectively masked by fatter, optically thick loops.

One further point that deserves discussion is the striking change in the appearance of the transition region between quiet Sun, where the emission is dominated by thin elongated structures, and active region plage, which is dominated by pointlike features (e.g., Fig. 1). The combined analysis of AR plage VAULT observations with *TRACE* 171 Å observations of the "moss," thought to be the 1 MK footpoints of overlying hot SXR coronal loops (e.g., Martens et al. 2000; Fletcher & De Pontieu 1999; Antiochos et al. 2003), indicated that it is possible that the Lyα emission seen by VAULT could originate from the footpoints of these loops like the "moss" (Vourlidas et al. 2001). This means that the different appearance the TR has in the quiet Sun is suggesting that the bulk of its emission comes from structures other than the footpoints of hot loops, and thus possibly from cool loops.

This is the first time a quantitative test for the existence of transition region cool loops has been carried out. Although this is definitely a significant step forward, we can think of several improvements to our study, before we can have a definitive result on the existence of cool loops. First, several simplifying assumptions of our model need to be relaxed. For instance, time-dependent effects could be important in cool loops (e.g., Spadaro

et al. 2006). VAULT movies show time variability on time-scales of 2–3 minutes. In addition, flows, resulting from either asymmetric steady heating or time-dependent heating, can have distinct spectroscopic signatures, which can help to distinguish between the competing possibilities for the origins, i.e., cool loops versus footpoints of hot loops, of the quiet Sun TR emission (e.g., Mariska 1987; Klimchuk & Mariska 1988; Spadaro et al. 2006). Third, subarcsecond spatial resolution high-sensitivity magnetic field observations (not available in our study) should reveal tiny magnetic bipoles in the sites of the postulated cool loops.

The most vigorous test for the existence of cool loops should involve subarcsecond spectroscopic observations in preferably optically thin transition region lines. This will avoid the complications of radiative transfer effects and will enable the inclusion of dynamics and flows in the relevant modeling, combined with matching spatial resolution high sensitivity photospheric magnetograms. The Very High Resolution Imaging Spectrometer (VERIS), for example, to be flown on a sounding rocket payload in 2008, will provide unprecedented spectroscopic observations in several transition region lines with a spatial resolution of $\approx 0.2''$ and a velocity discrimination better than 3 km s^{-1}. Such observations are expected to provide a further milestone in our understanding of the transition region.

Research supported by NASA and ONR. We thank for useful discussions J.-C. Vial, L. Teriaca, A.-H. Gabriel, P. Lemaire, J. T. Karpen, and J. Klimchuk for providing software and the referee for helpful suggestions.

REFERENCES

Aiouaz, T., & Rast, M. P. 2006, ApJ, 647, 183
Akiyama, S., Doschek, G. A., & Mariska, J. T. 2005, ApJ, 623, 540
Antiochos, S. K., Karpen, J. T., DeLuca, E. E., Golub, L., & Hamilton, P. 2003, ApJ, 590, 547
Antiochos, S. K., & Noci, G. 1986, ApJ, 301, 440
Athay, R. G. 1981, ApJ, 249, 340
Berger, T. E., et al. 2004, A&A, 428, 613
Berghmans, D., Clette, F., & Moses, D. 1998, A&A, 336, 1039
Bonnet, R. M., Bruner, E. C., Jr., Acton, L. W., Brown, W. A., & Decaudin, M. 1980, ApJ, 237, L47
Buchlin, E., Vial, J.-C., & Lemaire, P. 2006, A&A, 451, 1091
Chae, J., Schühle, U, & Lemaire, P. 1998, ApJ, 505, 957
Close, R. M., Parnell, C. E., Longcope, D. W., & Priest, E. R. 2004, ApJ, 612, L81
Dere, K. P. 1994, Adv. Space. Res., 14, 13
Dere, K. P., & Mason, H. E. 1993, Sol. Phys., 144, 217
Dere, K. P., et al. 1987, Science, 238, 1267
Doschek, G. A. 2006, ApJ, 649, 515
Doschek, G. A., Mariska, J. T., & Akiyama, S. 2004, ApJ, 609, 1153
Doschek, G. A., et al. 1998, ApJ, 507, 991
Dowdy, J. F., Rabin, D., & Moore, R. L. 1986, Sol. Phys., 105, 35
Feldman, U., Widing, K. G., & Warren, H. P. 1999, ApJ, 522, 1133
Fletcher, L., & De Pontieu, B. 1999, ApJ, 520, L135
Fontenla, J. M., Avrett, E. H., & Loeser, R. 1991, ApJ, 377, 712
Gabriel, A. H. 1976, Philos. Trans. R. Soc. London A, 281, 339
Gontikakis, C., Peter, H., & Dara, H. C. 2003, A&A, 408, 743
Gouttebroze, P. 2004, A&A, 413, 733
———. 2005, A&A, 434, 1165
———. 2006, A&A, 448, 367
Gouttebroze, P., Heinzel, P., & Vial, J.-C. 1993, A&AS, 99, 513
Griffiths, N. W., Fisher, G. H., Woods, D. T., & Siegmund, O. H. W. 1999, ApJ, 512, 992
Innes, D. E., Inhester, B., Axford, W. I., & Wilhelm, K. 1997, Nature, 386, 811
Klimchuk, J. A. 2000, Sol. Phys., 193, 53
Klimchuk, J. A., & Mariska, J. T. 1988, ApJ, 328, 334
Korendyke, C. M., et al. 2001, Sol. Phys., 200, 63
Landi, E., Mason, H. E., Lemaire, P., & Landini, M. 2000, A&A, 357, 743
Lemaire, P., Emerich, C., Curdt, W., Schühle, U., & Wilhelm, K. 1998, A&A, 334, 1095
Lemaire, P., Emerich, C., Vial, J.-C., Curdt, W., Schühle, U., & Wilhelm, K. 2005, Adv. Space Res., 35, 384
Mariska, J. T. 1987, ApJ, 319, 465
———. 1992, The Solar Transition Region (Cambridge: Cambridge Univ. Press)
Martens, P. C. H., Kankelborg, C. C., & Berger, T. E. 2000, ApJ, 537, 471
Patsourakos, S., & Vial, J. C. 2001, Sol. Phys., 203, 39
———. 2002, A&A, 385, 1073
Patsourakos, S., Vial, J. C., Gabriel, A. H., & Bellamine, N. 1999, ApJ, 522, 540
Peter, H. 2001, A&A, 374, 1108
Peter, H., Gudiksen, B. V., & Nordlund, A. 2004, ApJ, 617, L85
Reaves, E. M. 1976, Sol. Phys., 46, 53
Schrijver, C. J., & Title, A. M. 2003, ApJ, 597, L165
Schühle, U., Wilhelm, K., Hollandt, J., Lemaire, P., & Pauluhn, A. 2000, A&A, 354, L71
Spadaro, D., Lanza, A. F., Karpen, J. T., & Antiochos, S. K. 2006, ApJ, 642, 579
Teriaca, L., Banerjee, D., Falchi, A., Doyle, J. G., & Madjarska, M. S. 2004, A&A, 427, 1065
Tsiropoula, G. Alissandrakis, C., Bonnet, R. M., & Gouttebroze, P. 1986, A&A, 167, 351
Tu, C.-Y., Zhou, C., Marsch, E., Wilhelm, K., Zhao, L., Xia, L.-D., & Wang, J.-X. 2005, ApJ, 624, L133
Vourlidas, A., Klimchuk, J. A., Korendyke, C. M., Tarbell, T. D., & Handy, B. N. 2001, ApJ, 563,374
Wiegelmann, T., & Solanki, S. K. 2004, Sol. Phys., 225, 227
Winebarger, A. R., Emslie, A. G., Mariska, J. T., & Warren, H. P. 2002, ApJ, 565, 1298
Withbroe, G. L., & Noyes, R. W. 1977, ARA&A, 15, 363
Zachariadis, Th. G., Georgakilas, A. A., Koutchmy, S., Alissandrakis, C. E., & Dara, C. E. 1999, Sol. Phys., 184, 77